Recent Progress in Shell-Model Calculations for pfg-shell Nuclei

M. Honma[*], T. Otsuka[†], T. Mizusaki[**] and M. Hjorth-Jensen[‡]

[*]*Center for Mathematical Sciences, University of Aizu, Tsuruga, Ikki-machi, Aizu-Wakamatsu, Fukushima 965-8580, Japan*
[†]*Department of Physics and Center for Nuclear Study, University of Tokyo, Hongo, Bunkyo-ku, Tokyo 113-0033, Japan*
[**]*Institute of Natural Sciences, Senshu University, Higashimita, Tama, Kawasaki, Kanagawa 214-8580, Japan*
[‡]*Department of Physics and Center of Mathematics for Applications, University of Oslo, N-0316 Oslo, Norway*

Abstract. The structure of upper pf-shell nuclei is studied by the nuclear shell model, taking a model space consisting of four spherical single-particle orbits $p_{3/2}$, $f_{5/2}$, $p_{1/2}$ and $g_{9/2}$. The effective interaction JUN45 is used, which is obtained by modifying empirically the renormalized G-matrix interaction. The oblate-prolate shape coexistence in ^{68}Se is predicted consistently with the experimental observations, indicating the applicability of the shell model to the cases with moderate deformation. The calculated high-spin band structure highlights the important role played by the $g_{9/2}$ orbit. The appearance of the j_p-j_n multiplets in ^{88}Y is successfully described except for a few cases such as the 1^+_1 state, suggesting the good property of the effective proton-neutron interaction inherited from the renormalized G-matrix.

Keywords: Nuclear structure, Shell model
PACS: 21.60.Cs, 21.30.Fe, 27.50.+e, 27.60.+j

INTRODUCTION

In upper pf-shell nuclei, various interesting phenomena have been discovered recently, such as the development of nuclear deformation, the coexistence of different shapes near the ground state, the formation of isomeric states, the double β decay, and so on. In neutron-rich nuclei, the shell structure can be different from that of the stable nuclei, which reviles a new aspect of the nuclear tensor force [1]. From the astrophysical viewpoint, such a shell-evolution effect can affect the structure of the r-process nuclei and the nucleosynthesis. Thus, for a deeper understanding of these phenomena and reliable predictions of unobserved properties, it is desired to construct a theoretical model which can describe the upper pf-shell nuclei in a unified framework.

In this mass region, it is expected that the $g_{9/2}$ orbit plays a crucial role. This is a so-called unique-parity intruder orbit which is seen in the coexistence of low-lying opposite-parity states. Because of its high-j nature, it is sensitive to the deformation and the angular momentum, affecting the spin-dependent development of various shapes in low-lying states. The spin alignment of nucleons in this orbit can alter the high-spin band structure, and it also contributes to the formation of low-lying isomeric states. Therefore, it is essential to take into account the $g_{9/2}$ orbit explicitly and consider its relation to the upper pf-shell orbits.

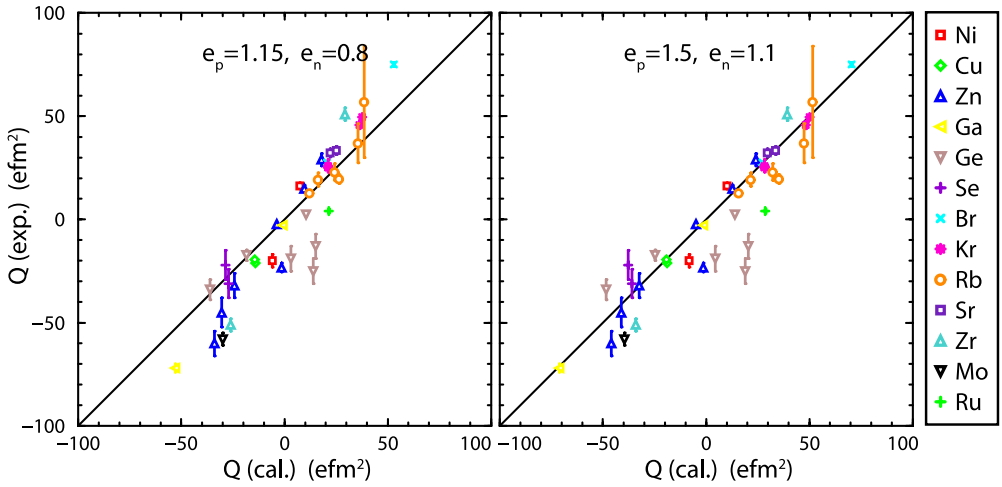

FIGURE 1. Comparison of quadrupole moments between the experimental data Q(exp.) and the calculation Q(cal.) with two sets of effective charges (e_p, e_n).

In this paper, we present our recent approach to this problem with the shell-model using the configuration space consisting of the four spherical single-particle orbits, $1p_{3/2}$, $0f_{5/2}$, $1p_{1/2}$, and $0g_{9/2}$ on top of an inert ^{56}Ni core (f5pg9-shell). One advantage of this choice is that it is free from the spurious center-of-mass motion. Moreover, although this model space is too large to carry out an exact diagonalization of the Hamiltonian matrix for the largest cases ($\sim$13 billion dimension in the M-scheme), for most of the nuclei considered in the present study, such an exact treatment is still possible by using the efficient shell-model code MSHELL [2].

EFFECTIVE INTERACTION

We use the effective interaction JUN45 [3] for shell-model calculations. This interaction was derived by modifying the realistic effective interaction G-f5pg9 (renormalized G-matrix [4] based on the Bonn-C potential) through the empirical fit to a body of experimental energy data. Such an approach has been successful for lighter-mass region such as the USD interaction [5, 6] for the sd-shell and the GXPF1 interaction [7, 8] for the pf-shell. The data to be fitted were selected so that we could expect relatively minor effects of the ^{56}Ni core excitations as well as the significant collectivity around the middle of the shell ($N\sim Z\sim 40$). The fitting was carried out iteratively by varying 45 well-determined linear combinations of 133 two-body matrix elements (TBME) and 4 single-particle energies (SPE). The mass number dependence $A^{-0.3}$ was assumed for the TBME as in the cases of the USD and the GXPF1. In the final fit, the rms deviation of 185 keV was attained between the experimental data and the shell model results.

The JUN45 interaction has been tested from various viewpoints such as the systematics of binding energies, magnetic dipole moments and electric quadrupole moments, low-lying energy levels, and so on. Figure 1 shows the comparison of quadrupole moments. In the left panel, the shell-model results are obtained with effective charges which

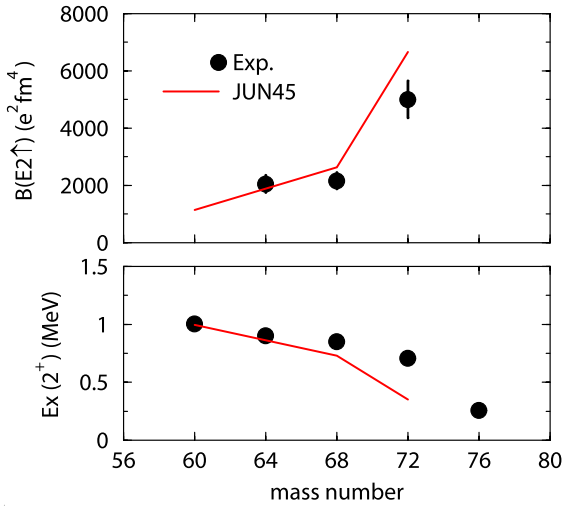

FIGURE 2. Comparison of (lower panel) excitation energies E_x (MeV) and (upper panel) $B(E2: 0_1^+ \rightarrow 2_1^+)$ (e^2fm^4) values between the experimental data (dots) and the shell-model results (lines) for N=Z even-even nuclei. The experimental data are taken from Refs. [10, 11, 12, 13]. The shell-model results for ^{72}Kr are obtained by an approximation method described in Ref. [14].

are suitable for the pf-shell space around ^{56}Ni [9]. It this case, the results systematically deviate from the diagonal line. On the other hand, in the right panel, we can see a reasonable agreement between the data and the shell-model results, where the effective charges are determined based on the least-squares fit to the experimental data. The adopted values (e_p, e_n)=(1.5, 1.1) are rather large, indicating the importance of the ^{56}Ni core polarization. We use the same effective charges in the following discussions.

TOWARDS DEFORMED REGION: N=Z NUCLEI

In N=Z nuclei, since the protons and neutrons occupy the same orbit, the strong proton-neutron interaction works efficiently, which can develop significant collectivity. As mentioned in the previous section, the JUN45 interaction was determined without any experimental data of nuclei around $N\sim Z\sim 40$ region in order to avoid possible difficulties for describing such collectivity due to the limited model space. Therefore, it is interesting to examine to what extent we can explore this region with the f5pg9-shell space.

For this purpose, it is useful to investigate the property of the first 2^+ state in even-even nuclei. It can be seen in Figure 2 that the shell-model results reasonably follow the experimental trend up to N=Z=34. However, for ^{72}Kr, the calculated $E_x(2^+)$ is too low in comparison with the experimental data, while the $B(E2)$ value from the ground state is somewhat too large. Thus, we can not expect a reasonable description of N=Z nuclei beyond $A\sim 70$ in the present shell model framework.

Next, we consider the structure of ^{68}Se (N=Z=34). According to the deformed potential model [15], the shape coexistence is predicted due to the existence of large single-particle energy gaps on both oblate and prolate side. Experimental observation [16, 17] is in fact consistent with the oblate ground state band, which is crossed by an excited

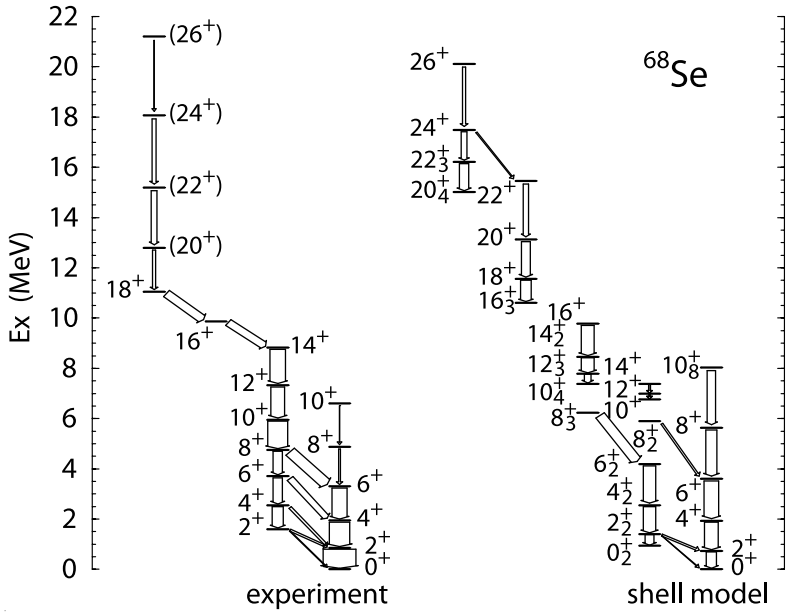

FIGURE 3. Comparison of energy levels between the experimental data and the shell-model results for ^{68}Se. The width of the arrow drawn in the experimental part corresponds to the relative γ-ray intensity, while it stands for the relative $B(\mathrm{E2})$ values in the theoretical part. Experimental data are taken from Refs. [16, 17].

band with prolate shape at around the spin $J\sim8$. For the description of such a structure, the interplay of the collective and the single-particle degrees of freedom should be properly taken into account. Although there are several approaches to this problem by the collective model or the mean-field model, the shell-model calculation based on the realistic interaction has been missing.

In Figure 3, the band structure is shown up to the excitation energy E_x=22MeV. In the shell-model results, we have obtained two low-lying bands on top of the 0^+_1 and the 0^+_2 states. The calculated quadrupole moment for the 2^+_1 is $+44e\mathrm{fm}^2$, and that for the 2^+_2 state is $-41e\mathrm{fm}^2$. This indicates that the ground band shows the oblate shape, while the excited band is prolate, which is consistent with the experimental findings. However, the calculated moment of inertia is somewhat too small especially in the prolate band. As a result, the crossing with the oblate band never occurs. This indicates the insufficient collectivity for the prolate deformation within the present model space.

Experimentally, the prolate band is extended up to spin J=26. The shell-model results predict the development of such a prolate band, showing a reasonable correspondence with the experimental data. It is interesting to note that, the calculated band structure is characterized by the occupation number of the $g_{9/2}$ orbit. In the ground-state oblate band and the low spin (J=0$\sim$8) excited prolate band, this number is about one. For the intermediate spin (J=10$\sim$14) and the high spin (J=16$\sim$22) members of the prolate band, this number it is about 2.3 and 4.1, respectively. Thus, the higher spin bands are generated by successive promotions of nucleons into the $g_{9/2}$ orbit. These numbers are almost constant within these spin ranges, suggesting the stability of the intrinsic structure. Considering the reasonable overall agreement between the experimental data

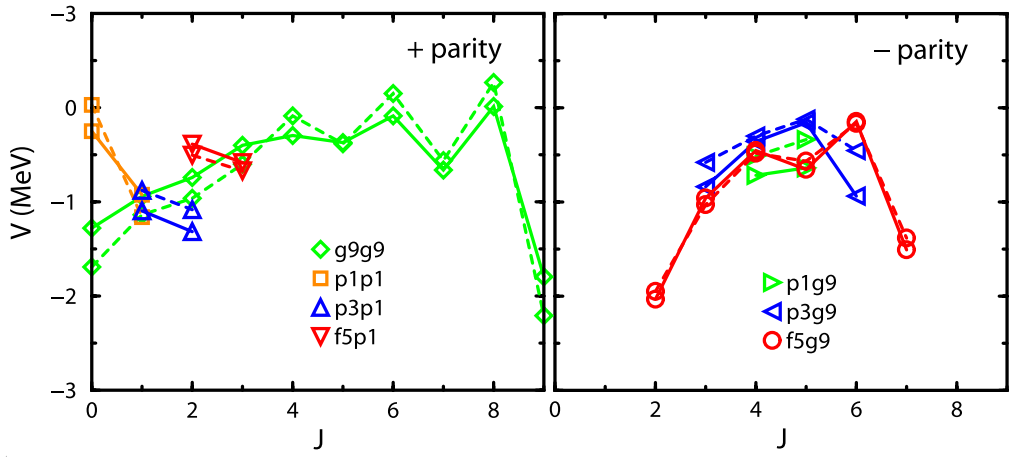

FIGURE 4. Comparison of the proton-neutron two-body diagonal matrix element $\langle j_\pi j'_\nu \,|V|\, j_\pi j'_\nu \rangle_J$ as a function of the angular momentum J between the G-f5pg9 (solid lines) and the JUN45 (dashed lines) interactions. The label "p1g9" stands for j_π=$\pi p_{1/2}$ and j'_ν=$\nu g_{9/2}$, for example.

and the shell-model results, we can expect that the JUN45 successfully describes the single-particle properties related to the $g_{9/2}$ orbit in the deformed mean potential.

PROTON-NEUTRON MULTIPLETS STRUCTURE

The proton-neutron interaction can be investigated through the structure of odd-odd nuclei around the shell closure. In the energy spectra, we can find a characteristic feature due to the coupling of the unpaired proton and neutron in the orbit j_π and j_ν, respectively, which is directly related to the proton-neutron TBME. It should be noted that, the differences between the JUN45 interaction and the original G-f5pg9 interaction due to the empirical fit are mainly in the monopole part and in the T=1 pairing matrix elements. In other words, the multipole part of the TBME, especially the J dependence of the proton-neutron diagonal TBME is quite similar between the JUN45 and the G-f5pg9, as shown in Figure 4. Therefore, the proton-neutron multiplet structure predicted by the JUN45 inherits the property of the microscopic G-matrix interaction.

As an example, we consider ^{88}Y, for which the low-lying energy levels are shown in Figure 5. It has been known that this nucleus can successfully be described as a one-proton-particle-one-neutron-hole state on top of the ^{88}Sr inert core. Based on this picture, various shell-model analysis have been published by using the model space consisting of only two orbits $p_{1/2}$ and $g_{9/2}$ (p1g9-shell). In the same Figure, two examples of such an approach by Gross et al. [18] and by Serduke et al. [19] are shown. By comparing them with the results of the JUN45 obtained in the extended model space including the $p_{3/2}$ and $f_{5/2}$ orbits, we can examine the validity of such a simple picture.

In the energy spectra obtained by the shell model with the JUN45 interaction, one can find several j_π-j_ν multiplets. For example, the calculated wavefunctions of the 4^-_1-5^-_1 states are dominated by the $\pi(p_{1/2})^1\nu(g_{9/2})^{-1}$ configuration with about 60% probability. Also, the 4^+_1-5^+_1-6^+_1-7^+_1-8^+_1-9^+_1 states are of the $\pi(g_{9/2})^1\nu(g_{9/2})^{-1}$ character

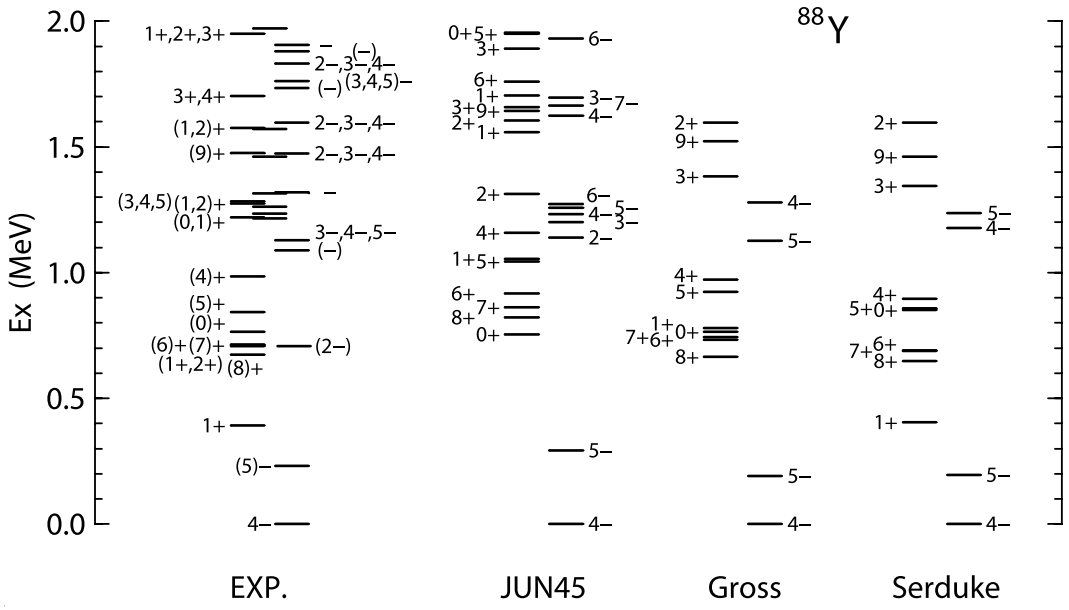

FIGURE 5. Energy levels of ^{88}Y. Experimental data (EXP.) are compared with the shell-model results obtained by using three effective interactions: JUN45 [3], the interaction derived by Gross et al. [18], and that by Serduke et al. [19]. In each case, the positive (negative) parity states are drawn in the left (right) column. In the experimental data, several states with no parity assignment are shown between these two columns. Experimental data are taken from Ref. [10].

($\sim$ 50%). For these states, the agreement between the experimental data and all the three shell-model results looks rather good, suggesting the validity of the approaches within the p1g9-shell. However, as for the 4_2^--5_2^- doublets, the configuration within the p1g9-shell is only about 25%, and many other configurations can be found in the calculated wavefunctions. Also, there are several states at around $E_x\sim$1.2MeV or higher, which are missing in the shell-model results of the p1g9-shell. The experimental spin assignment is desired for these states to clarify the contribution of configurations outside the p1g9-shell and to evaluate the predictions by the JUN45 interaction.

We can find a remarkable difference between the experimental data and the JUN45 prediction in the 1_1^+ state. Note that this state appears at the reasonable excitation energy in the results by Serduke et al, while it is relatively closer to that of the JUN45 in the results by Gross et al. In these two p1g9-shell calculations, the effective interaction was determined by a direct fit to the experimental energy levels. However, in the former, this 1_1^+ state was included in the data to be fitted, while it was not in the latter. According to Gross et al, the fitting to this 1_1^+ state demands a significant breaking of the charge independence in the effective interaction. Since we assume the isospin symmetry in the JUN45 interaction, the similarity between the results of the JUN45 and Gross et al is reasonable. In a naive picture, this 1_1^+ state consists mainly of the $\pi(p_{1/2})^1\nu(p_{1/2})^{-1}$ configuration. It was expected that the explicit treatment of the $p_{3/2}$ and $f_{5/2}$ orbits might improve the description of this 1_1^+ state through the mixing with the configurations such as $\pi(p_{1/2})^1\nu(p_{3/2})^{-1}$. However, in the JUN45 results, such a component is only 1% in

the 1_1^+ state, and there is no improvement in the agreement with the experimental data. It may be needed to extend the model space further to describe this state. For example, a possible pairing excitation from the $\nu g_{9/2}$ orbit may lower the $\pi(p_{1/2})^1\nu(p_{1/2})^{-1}$ multiplets relative to the $\pi(g_{9/2})^1\nu(g_{9/2})^{-1}$ ones, improving the description.

SUMMARY

In summary, the structure of the upper pf-shell nuclei was studied by the shell-model framework in the f5pg9-shell. In spite of the modest size of the model space, the JUN45 interaction describes rather well the collective features along the $N = Z$ line up to $A\sim70$. The predicted shape coexistence and the high-spin band structure in ^{68}Se are in reasonable agreement with the experimental data, suggesting the successful description of the deformed single-particle properties related to the $g_{9/2}$ orbit. The structure of ^{88}Y can be interpreted in terms of the j_π-j_ν multiplets. The reasonable agreement between the shell-model results and the experimental data implies the validity of the multipole part of the adopted proton-neutron interaction, which is largely inherited from the microscopic G-matrix interaction.

ACKNOWLEDGMENTS

This work has been a part of the CNS-RIKEN joint research project on large-scale nuclear-structure calculations. This work was supported in part by a Grant-in-Aid for Scientific Research (A) (20244022) from the MEXT, and also by the JSPS core-to-core program "International Research Network for Exotic Femto Systems (EFES).

REFERENCES

1. T. Otsuka, T. Suzuki, R. Fujimoto, H. Grawe and Y. Akaishi, Phys. Rev. Lett. **95**, 232502 (2005).
2. T. Mizusaki, RIKEN Accel. Prog. Rep. **33**, 14 (2000).
3. M. Honma, T. Otsuka, T. Mizusaki, and M. Hjorth-Jensen, Phys. Rev. C **80**, 064323 (2009).
4. M. Hjorth-Jensen, T. T. S. Kuo and E. Osnes, Phys. Repts. **261**, 125 (1995).
5. B. A. Brown and B. H. Wildenthal, Ann. Rev. Nucl. Part. Sci. **38**, 29 (1988).
6. B. A. Brown and W. A. Richter, Phys. Rev. C **74**, 034315 (2006).
7. M. Honma, T. Otsuka, B. A. Brown and T. Mizusaki, Phys. Rev. C **65**, 061301(R) (2002).
8. M. Honma, T. Otsuka, B. A. Brown and T. Mizusaki, Phys. Rev. C **69**, 034335 (2004).
9. R.du Rietz *et al.*, Phys. Rev. Lett. **93**, 222501 (2004).
10. Data extracted using the NNDC WorldWideWeb site from the ENSDF database.
11. K. Starosta *et al.*, Phys. Rev. Lett. **99**, 042503 (2007).
12. A. Obertelli *et al.*, Phys. Rev. C **80**, 031304(R) (2009).
13. A. Gade *et al.*, Phys. Rev. Lett. **95**, 022502 (2005).
14. M. Honma, B. A. Brown, T. Mizusaki and T. Otsuka, Nucl. Phys. **A704**, 134c (2002).
15. W. Nazarewicz *et al.*, Nucl. Phys. **A435**, 397 (1985).
16. S. M. Fischer *et al.*, Phys. Rev. Lett. **84**, 4064 (2000).
17. S. M. Fischer, C. J. Lister and D. P. Balamuth, Phys. Rev. C **67**, 064318 (2003).
18. R. Gross and A. Frenkel, Nucl. Phys. **A267**, 85 (1976).
19. F. J. D. Serduke, R. D. Lawson and D. H. Gloeckner, Nucl. Phys. **A256**, 45 (1976).